Sawtooth activity of the ion cloud in an electron-beam ion trap

R. Radtke and C. Biedermann
Bereich Plasmadiagnostik, Max-Planck-Institut für Plasmaphysik, EURATOM Association, D-10117 Berlin, Germany
(Received 13 November 2002; published 12 March 2003)

The dynamics of an ensemble of highly charged Ar and Ba ions in an electron-beam ion trap (EBIT) was studied by recording time-resolved x-ray spectra emitted from trapped ions. Sawtoothlike signatures manifest in the spectra for a variety of EBIT operating conditions indicating a sudden collapse of the ion inventory in the trap. The collapse occurs on a time scale of approximately 100 ms and the evolution of the sawteeth is very sensitive to parameters such as electron-beam current and axial trap depth. Analysis of the measurements is based on a time-dependent calculation of the trapping process showing that sawtooth activity is caused by the feedback between the low-Z argon and high-Z barium ions. This unexpected behavior demonstrates the importance of nonlinear effects in electron-beam traps containing more than a single ion species.

DOI: 10.1103/PhysRevA.67.032705 PACS number(s): 34.80.Dp, 29.25.Ni, 39.10.+j, 52.58.Qv

The evolution of ions in an electron-beam ion trap (EBIT) is a complex interplay of a large number of processes. It depends on the dynamics of ion creation and heating as well as on such factors as trap potential and beam energy or the type of trap seeding. Information about the process is of importance in understanding the trapping conditions in the EBIT itself and, in addition, for applications extending from atomic physics measurements to using the trap inventory as a source of ions for external experiments. A description of the EBIT technique is given elsewhere [1,2] and here we emphasize only the wide variety of elements and charge states available for investigation [3]. To understand the details in which ions evolve in an EBIT, several computer codes have been developed [4–8] and applied in a number of cases to provide estimates of charge balance and temperature for confined ions. However, the predictive quality of the results is limited, not only because of uncertainties in the atomic physics data, but also because of deficiencies in the EBIT models. A problem of this nature, for example, is that of ion-space charge effects, which are completely neglected in the existing codes. Measurement of the evolution of ions was made early on [4,9–11] as well as late [12,13] in the experiment. While the emphasis in Refs. [4,9–11] was on determining the ions' development toward equilibrium, in Refs. [12,13] it was on providing trapping lifetimes for confined ions and demonstrating the effect of evaporative cooling by low-Z atoms.

In this paper we report on the evolution of ions in an EBIT while feeding the trap with a constant flux of a lighter (argon, $Z=18$) and a heavier element (barium, $Z=56$). Working with a mixture of different ions with different charge states resembles what is termed ''evaporative cooling'' in electron-beam ion sources and traps [1]. Evaporative cooling is the key to the successful operation of an EBIT and has been proven to be necessary for the breeding of very highly charged ions. The present investigation relies on an unusual variation of this technique: The rate at which the light component (coolant gas) is injected into the trap was much larger than the influx of the heavy component. By operating the EBIT in this way we could observe the excitation of sawtoothlike features being caused by a periodic collapse of the ion population in the trap. Up to now, neither have measurements of such signatures in an EBIT been made nor have they been predicted by theoretical calculations. Perhaps most importantly, the wave form of the sawtooth spectrum is very sensitive to electron-beam current and axial trap depth, and there are thresholds for switching the activity on and off. These properties are quite unique and suggest the possibility of using sawtooth oscillations as benchmark data to test existing EBIT models. Other low-density plasma devices where sawtooth oscillations have been observed from early on are tokamak facilities [14]. Without going into the details, we mention that sawtooth activity in a tokamak has the nature of a hydromagnetic relaxation instability [15].

Our measurements in EBIT were carried out for a mixture of Ar and Ba ions. Argon was introduced into the trap by means of a gas injector system while barium is an EBIT-intrinsic contaminant given off by the heated electron-gun cathode. The EBIT was operated in a static mode where all experimental conditions were held constant after closing the trap at $t=0$. Typical electron-beam currents were $I_b=50$ mA; the electron-beam energy was fixed throughout the measurements at $E_b=5.0$ keV, limiting the maximum charge of Ar to $18+$ and of Ba to $46+$. The time evolution was monitored for as long as 50 s by recording the characteristic x-ray emission from the trapped ions. We have measured the radiation in the region above ~ 500 eV using a solid-state Ge detector. The x rays were recorded in event-time mode with a resolution of 50 ms. These data can be presented as a scatter plot, as illustrated in Fig. 1. In the plot the x rays registered from all particles trapped in EBIT are traced as a function of time. Emission bands for Ar and Ba from different x-ray production mechanisms are marked. A prominent feature is the time structure of the x-ray emission showing that the population does not reach a steady state. The signal for Ba increases steadily over successive time periods while the intensity of Ar, acting as coolant, diminishes. Towards the end of each period a sudden decline in the signal is observed in all radiation channels indicating a collapse of the ion inventory in the trap. The collapse occurs on a time scale of approximately 100 ms and restores the initial conditions for a new start-up of the process. Looking beyond the 25-s-wide window of Fig. 1 showed that the effect even persisted for 10 min, the longest exposure used in our investigation.

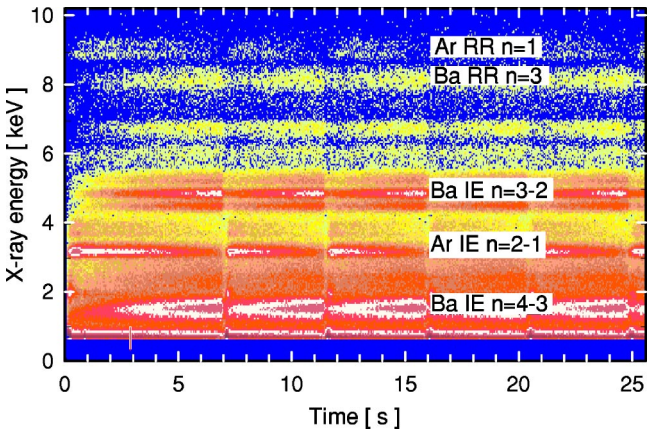

FIG. 1. X-ray emission vs time after closing the trap at $t=0$. All operating parameters were kept constant during the 25-s recording time ($E_b=5.0$ keV, $I_b=50$ mA, $\Delta V_{ax}=15$ V). The traces between about 1- and 5-keV x-ray energy represent impact excitation (IE) of Ar and Ba lines. The x-ray events above 5 keV result from radiative recombination (RR) into $n\geqslant 1$ shells for Ar and $n\geqslant 3$ shells for Ba.

We have measured the evolution of ions for several different electron-beam currents I_b and axial trap depths ΔV_{ax} covering the range of 20–70 mA and 2–300 V, respectively. $\Delta V_{ax}=V_{bias}+V_{ip}$ is the sum of the upper drift tube's bias and the image potential formed by the electron beam and the geometry of the trap $V_{ip}\simeq 0.14(I_b\sqrt{m_e}/\epsilon_0\sqrt{E_b})$. Time traces for Ar and Ba were constructed by applying cuts to data plots similar to Fig. 1 along the Ar IE $n=2-1$ and Ba IE $n=3-2$ bands and projecting the x-ray events found in these cuts onto the time axis. Representative graphs of time profiles for different conditions are shown in Figs. 2 and 3. Figure 2 presents data sets showing the effect of ΔV_{ax} on the profiles. For a shallow trap with an axial potential of 2 V the Ar ions essentially escape immediately after being created while the intensity of the Ba ions increases and levels to a plateau. As the trap is made deeper a significantly greater amount of x-ray emission is observed equivalent to greater abundances of ions confined in the trap. Raising ΔV_{ax} thus implies that the collision rate and accordingly the exchange between the ions is progressively enhanced. In the 4-V plot a situation is shown whereby a threshold for the excitation of sawteeth is reached. Evidence for this are the small oscillations in the Ar and Ba intensities at early confinement times. The growth of the sawteeth as ΔV_{ax} is further raised is seen in the 9-V and 15-V plots. Notice also how with higher potentials the system takes longer to reach sawtooth activity. For potentials above approximately 20 V there is a drastic change in the qualitative appearance of the time profiles; the sawtooth activity is weakening and a transition occurs to a new mode where the periodic mechanism is definitely turned off after the ion cloud's first collapse. We stress here that this single ion expulsion is observed even during routine and normal EBIT operation, while the periodic sawtooth mechanism requires special trapping conditions (shallow trap).

Time profiles as a function of the electron-beam current are shown in Fig. 3. Since the bias voltage V_{bias} was held constant for the I_b scan and because of $V_{ip}\propto I_b$, the axial

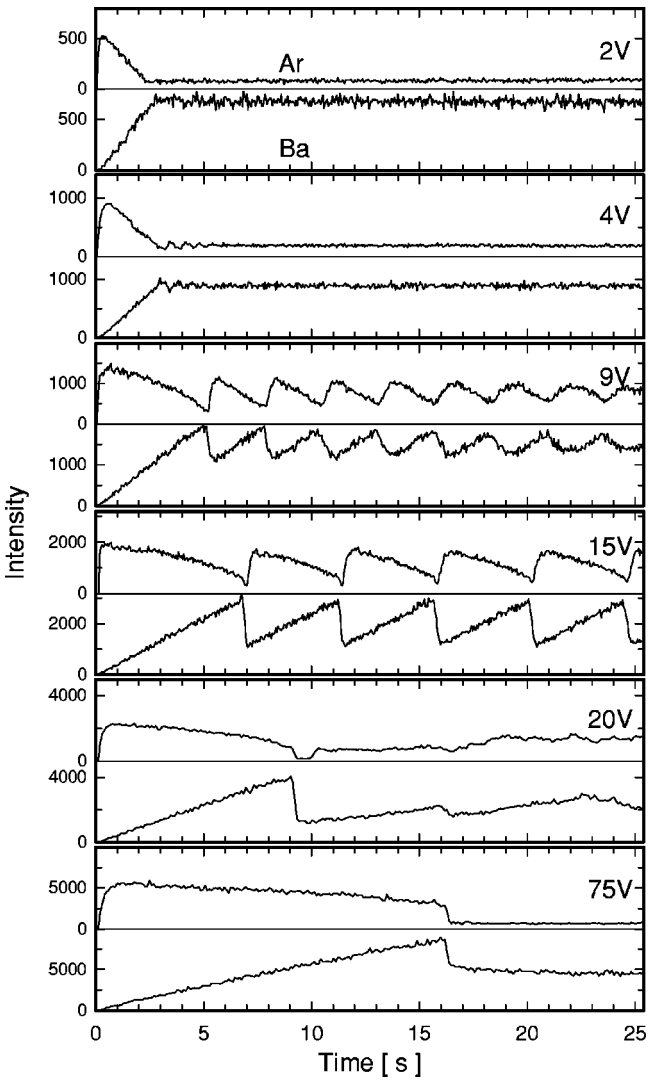

FIG. 2. Time profile of $n=2-1$ and $n=3-2$ emission spectra of Ar and Ba for six axial trap depths ΔV_{ax}. The value of ΔV_{ax} is plotted in each panel showing the Ar trace. The beam current and energy are fixed parameters ($I_b=50$ mA, $E_b=5.0$ keV).

potential $\Delta V_{ax}=V_{bias}+V_{ip}$ changes with I_b as indicated in the caption. Most prominent is the strong variation in the time structure and the extinction of the sawtooth activity when I_b decreased below 49 mA. The shortening tooth length is due to the trap potential decreasing with I_b. This is also obvious in Fig. 2 where the effect is more pronounced because of the larger variation in ΔV_{ax}. The data in Fig. 3 display larger tooth lengths than expected from the ΔV_{ax} scan of Fig. 2. The explanation is that the scans were taken two weeks apart with different conditions for the injection of Ba from the electron gun. We have measured time profiles at different gas injection pressures and could confirm the observed feature, i.e., the variation of the tooth length with the particle influx.

In order to provide an explanation for the sawtooth mechanism, modeling of the time evolution of Ar and Ba ions has been carried out for conditions similar to those used in the experiment. The description includes (a) electron-

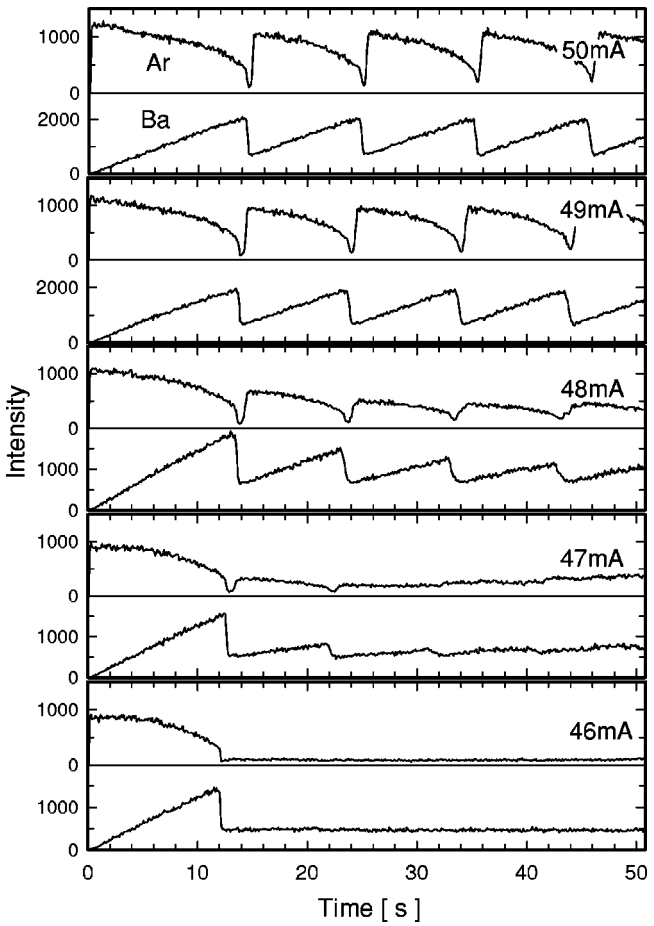

FIG. 3. Time profile of $n=2-1$ and $n=3-2$ emission spectra of Ar and Ba for five beam currents ($I_b=46-50$ mA). The beam energy was $E_b=5.0$ keV and the upper drift tube's bias was held at $V_{bias}=-10$ V. The values of ΔV_{ax} determined from these settings are 15.5, 15.0, 14.5, 14.0, and 13.5 V, in order of decreasing current.

impact ionization and (b) electron-beam heating of the ions, (c) ion-ion energy exchange, (d) axial ion escape from the trap, (e) radial overlap factors (electron-ion and ion-ion), and (f) trap neutralization by ions. For simplicity we assume constant density of neutrals for Ar and Ba and consider each element to be capable of populating only a representative sequence of charge states: $q=1, 2, 5, 10, 16, 17, 18$ for Ar and $q=1, 3, 6, 10, 23, 38, 46$ for Ba. These states were selected to cover the time scale for low as well as highly charged ion production, extending from 10^{-6} s to 1 s. We note that covering the complete time scale is essential to warrant the dynamics of ion creation and picking only two representatives of each component did not enable us to simulate any oscillations. A set of 28 coupled rate equations for the ion density and temperature was used to determine the time evolution, viz.,

$$\frac{dN_{\alpha,i}}{dt}=\frac{N_{\alpha,i-1}}{\tau^{ion}_{\alpha,i-1}}-\frac{N_{\alpha,i}}{\tau^{ion}_{\alpha,i}}-\frac{N_{\alpha,i}}{\tau^{con}_{\alpha,i}}, \quad (1)$$

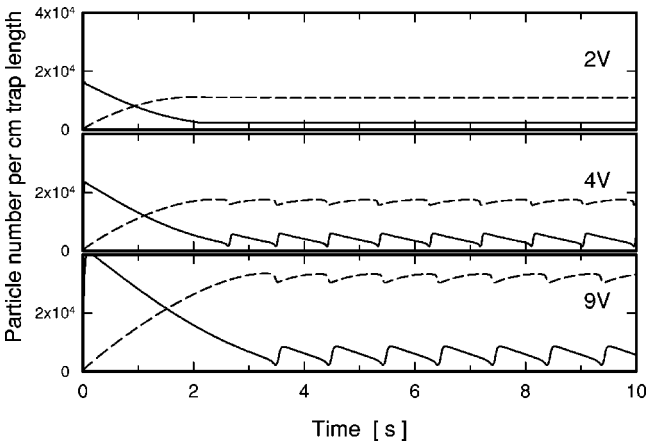

FIG. 4. Calculated time evolution of $N_{\mathrm{Ar}}=\Sigma_i N_{\mathrm{Ar},i}$ (solid line) and $N_{\mathrm{Ba}}=\Sigma_i N_{\mathrm{Ba},i}$ (dashed line) at $\Delta V_{ax}=2$, 4, and 9 V, respectively. Beam current and energy are as for Fig. 2. The calculations are based on Eqs. (1) and (2) and assume $N_{\mathrm{Ar},0}=8.2$ and $N_{\mathrm{Ba},0}=0.1$ per cm trap length.

$$\frac{d}{dt}\left(\frac{3}{2}kT_{\alpha,i}N_{\alpha,i}\right)=\frac{dW^{b}_{\alpha,i}}{dt}-\frac{dW^{d}_{\alpha,i}}{dt}+\sum_j\left(\frac{dW^{c}_{\alpha,i}}{dt}\right)_j. \quad (2)$$

$N_{\alpha,i}$ is the total number of trapped ions ($\alpha=$ Ar, Ba) in charge state q_i, $\tau^{ion}_{\alpha,i-1}$ the characteristic time to create the charge state q_i, and $\tau^{con}_{\alpha,i}$ the ion confinement time. Equation (2) states that the ion temperature $T_{\alpha,i}$ is obtained from the balance between heating and cooling taking the processes (b), (c), and (d) into account; the sum is over all Ar and Ba charge states in question. For $\tau^{con}_{\alpha,i}$ and the energies $W^{b,\,c,\,d}_{\alpha,i}$ in Eqs. (1) and (2) we have employed the definitions from Ref. [16]. The effect of trap neutralization was incorporated by adding the ions' potential V_{ion} to the trap depth ΔV_{ax}. Values of V_{ion} were calculated from the predicted number and characteristic radius $r_{\alpha,i}$ of the confined ions assuming constant ion-density distributions for $r<r_{\alpha,i}$. To begin with we calculated time profiles $N_{\alpha,i}(t)$ as a function of $N_{\mathrm{Ar},0}$ and $N_{\mathrm{Ba},0}$, the number of neutrals in the beam, for the parameters of the 2-V plot in Fig. 2. With regard to the condition $N_{\mathrm{Ba},0}\ll N_{\mathrm{Ar},0}$ we adjusted $N_{\mathrm{Ar},0}$ and $N_{\mathrm{Ba},0}$ in the calculation until the time structure of the experimental spectrum was reproduced. Based on these numbers a set of calculations has then been made to predict time profiles for a range of ΔV_{ax} values. Time histories for three trap depths are shown in Fig. 4. In Fig. 5 the predicted ion temperatures and total rates $\dot{N}_\alpha=(d/dt)\Sigma_i N_{\alpha,i}$ are shown for a typical sawtooth.

Although our computations rely on a fairly incomplete model, they contain the interplay between the argon and barium ions and exhibit features that are quite similar to part of the experimental findings. From the data calculated in Figs. 4 and 5, the tooth mechanism can clearly be identified: Initially the strong cooling effect of Ar dominates and Ba ions accumulate in the trap at slightly increasing temperature. The number of argon ions is decreasing at this stage of evolution ($\dot{N}_{\mathrm{Ar}}<0$ and $\dot{N}_{\mathrm{Ba}}>0$). As the populations evolve a situation is approached where the benefit of cooling is considerably reduced due to the reduction of N_{Ar} and the Ba ions

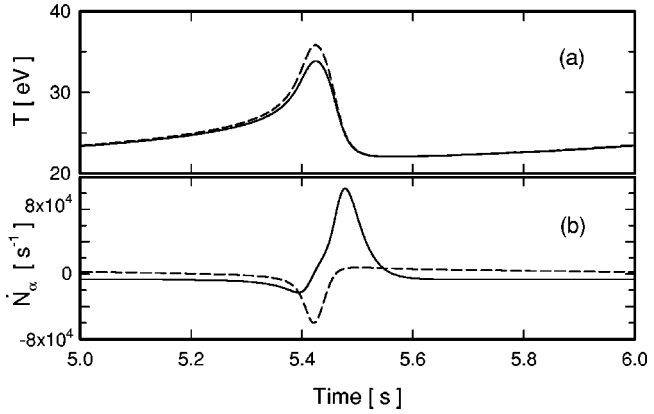

FIG. 5. Details of the calculated time evolution during the rise and fall periods of a typical sawtooth. In (a) the ion temperatures of Ar^{18+} (solid line) and Ba^{46+} (dashed line) are plotted. (b) shows the total rates $\dot{N}_\alpha$ for Ar (solid line) and Ba (dashed line). Parameters as for Fig 4, $\Delta V_{ax}=9$ V.

encounter substantially more heating. This accelerates the temperature increase and particle loss from the trap and therefore N_{Ba} is changed from an increasing to a decreasing function of time ($\dot{N}_{\mathrm{Ba}}<0$). As N_{Ba} (and N_{Ar}) falls the temperature increase is further accelerated [because $dW^d_{\alpha,i}/dt$ in Eq. (2) is strongly reduced at lower ion density] and the rates $\dot{N}_\alpha$ progressively change. It is important to note that this change in behavior of the $\dot{N}_{\mathrm{Ar}}$ and $\dot{N}_{\mathrm{Ba}}$ curves is in large part due to a diminishing ion-ion collision rate ($\nu_i \propto n_i/T_i^{3/2}$) which prevents the ions from equilibrating their temperatures. The point $\dot{N}_{\mathrm{Ba}}=\dot{N}_{\mathrm{Ar}}$ marks the time where the Ar density and temperature begin to stabilize and the sawtooth mechanism is started in the trap. In fact, once the rates have intersected as a function of time, the decrease in N_{Ba} is faster than that in N_{Ar}. This slows down the rate at which energy is transferred from the higher-charge-state Ba ions to the Ar ions allowing the latter to stay in the electron beam longer. The rise in the $\dot{N}_{\mathrm{Ar}}$ curve in Fig. 5(b) is a consequence of improved storage. For conditions where $\dot{N}_{\mathrm{Ar}}>0$ an increasing number of Ar ions is accumulated in the trap. They are heated less by the electron beam and cool the Ba ions at declining temperature until $\dot{N}_{\mathrm{Ba}}$ and thus N_{Ba} become high enough to allow the competition between Ar and Ba to recommence.

Figure 4 shows calculated time histories $N_\alpha(t)$ that behave qualitatively similarly to the profiles measured at the lower trapping potentials (see Fig. 2). The calculations accurately predict the time scales of the quickly increasing and decreasing intensity and indicate when sawtooth activity does or does not occur. As expected and demonstrated in the figure, the effect requires favorable conditions and becomes present at increased density (i.e., higher ion-ion collision rate) when the Ar and Ba ions are well mixed by collisions. However, the calculations did not reproduce the strength of the ion collapse in the trap and accordingly the tooth lengths measured or the threshold behavior observed in the time profiles at $\Delta V_{ax}>20$ V (Fig. 2) and $I_b<48$ mA (Fig. 3). This underlines the complexity of the ion dynamics in EBIT which is difficult to predict with simple assumptions. The origin of this discrepancy is not well understood. It is likely that this difference is related to the problem of finding the potential from the trapped ions. This potential plays an important role since it causes the true axial trap depth to deviate from ΔV_{ax}. The values for V_{ion} in the present simulation (up to 20% of ΔV_{ax}) provide an indication of the effect, but they may not be a good estimate over an extended range of ion temperature and density. An improvement in V_{ion} determination is achieved by adding Poisson's equation to Eqs. (1) and (2) and finding self-consistent solutions for the ion potential. However, this would require much more computing effort which is beyond the scope of the present analysis. Preliminary calculations were made to infer the effect that an alternative treatment could have on the sawtooth spectrum. We adopted an approach in which the ion cloud is regarded to undergo a contraction during the accumulation process. A contraction of the ion cloud is predicted from the self-consistent solution for the combined space-charge potentials of the electron beam and the trapped ions [16]. It can occur when ions concentrate in the trap during extended accumulation and the beam-neutralization factor approaches 1. The trapping potential and ion temperature in this case decrease dramatically and a transition to an open trap regime can take place. The effect could disable the periodic oscillations and thus explain the thresholds observed in Figs. 2 and 3.

In summary, we report on the observation of sawtooth activity in an electron-beam-ion trap caused by the feedback between ions of a light and heavy element. This two-component ion plasma is a genuine example of a complex dynamical system interacting in highly nonlinear manner. Results from numerical calculations clearly identify the basic mechanism and indicate that the effect might enable the preparation of a large number of highly charged, cold ions. The features observed in the sawtooth spectrum represent an excellent tool for testing theoretical EBIT models and probing the dynamics in ion traps and sources.

We would like to thank G. Fussmann for many helpful and stimulating discussions during the course of this work.

[1] M.A. Levine, R.E. Marrs, J.R. Henderson, D.A. Knapp, and M.B. Schneider, Phys. Scr. T **22**, 157 (1988).

[2] F. J. Currell, in *Trapping Highly Charged Ions: Fundamentals and Applications*, edited by J. Gillaspy (Nova Science Publishers, New York, 2001), p. 3.

[3] R.E. Marrs, S.R. Elliott, and D.A. Knapp, Phys. Rev. Lett. **72**, 4082 (1994).

[4] B.M. Penetrante, J.N. Bardsley, D. DeWitt, M. Clark, and D. Schneider, Phys. Rev. A **43**, 4861 (1991).

[5] B.M. Penetrante, J.N. Bardsley, M.A. Levine, D.A. Knapp, and

R.E. Marrs, Phys. Rev. A **43**, 4873 (1991).
[6] H. S. Margolis, Ph.D. thesis, Pembroke College Oxford, 1994 (unpublished).
[7] P. Liebisch, diploma work, Humboldt University, Berlin, 1998 (unpublished).
[8] I.V. Kalagin, D. Küchler, V.P. Ovsyannikov, and G. Zschornack, Plasma Sources Sci. Technol. **7**, 441 (1998).
[9] C. Biedermann, T. Fuchs, P. Liebisch, R. Radtke, E. Behar, and R. Doron, Phys. Scr. T **80**, 303 (1999).
[10] J.V. Porto, I. Kink, and J.D. Gillaspy, Rev. Sci. Instrum. **71**, 3050 (2000).
[11] F.J. Currell, H. Kuramoto, S. Ohtani, C. Scullion, E.J. Sokell, and H. Watanabe, Phys. Scr. T **92**, 147 (2001).
[12] M.B. Schneider, M.A. Levine, C.L. Bennett, J.R. Henderson, D.A. Knapp, and R.E. Marrs, in *International Symposium on Electron Beam Ion Sources and Their Application*, edited by A. Hershcovitch, AIP Conf. Proc. 188 (AIP, New York, 1989), p. 158.
[13] C. Biedermann, T. Fuchs, G. Fussmann, and R. Radtke, in *Trapping Highly Charged Ions: Fundamentals and Applications*, edited by J. Gillaspy (Nova Science Publishers, New York, 2001), p. 80.
[14] S. von Goeler, W. Stodiek, and N. Sauthoff, Phys. Rev. Lett. **33**, 1201 (1974).
[15] J. Wesson, *Tokamaks* (Clarendon Press, Oxford, 1987).
[16] G. Fussmann, C. Biedermann, and R. Radtke, in *Advanced Technologies Based on Wave and Beam Generated Plasmas*, edited by H. Schlüter and A. Shivarova (Kluwer Academic Publishers, Dordrecht, 1999), p. 429.